

ROBUST CAPACITIVE MEMS ULTRASONICS TRANSDUCERS FOR LIQUID IMMERSION

D.W. Greve and J.J. Neumann

Department of Electrical and Computer Engineering, Carnegie Mellon University, Pittsburgh, PA, USA

I.J. Oppenheim

Department of Civil and Environmental Engineering, Carnegie Mellon University, Pittsburgh, PA, USA

S.P. Pessiki and D. Ozevin

Dept. of Civil and Environmental Engineering, Lehigh University, Bethlehem, PA, USA

Abstract - Capacitive diaphragm MEMS ultrasonic transducers are of great interest because they offer wide bandwidth and ready integration into arrays. However, fragility of these transducers is a significant barrier to their application. In this talk, we report on robust transducers which have been fabricated using the MUMPS process. The transducer design has been optimized to minimize stray capacitance between the output node and the substrate. We report the use of a protective silicone layer which protects the transducers from liquid exposure and, to a degree, from mechanical damage. The silicone layer has been applied with high transducer yield without the need for prior closure of the etch holes, and coated transducers survive extended immersion in water. The thickness of the silicone layer must be carefully controlled, however, in order to prevent pulse distortion.

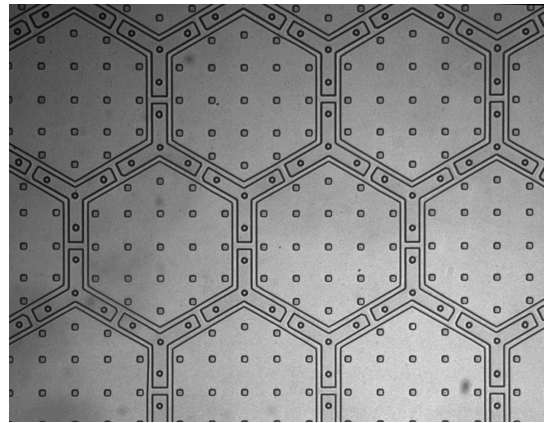


Fig. 1. Optical micrograph of transducer (design B).

I. INTRODUCTION

MEMS ultrasonic transducers (sometimes termed cMUTs, for capacitive MEMS Ultrasonic Transducers), have been studied by several research groups [1,2,3,4,5,6] both for liquid immersion applications [1,2,3,4] and also in contact with solid media [5,6]. In many of these applications fragility of the transducers is an important issue. Here, we will report on the use of a thin silicone coating to provide acoustic coupling, electrical insulation, and a degree of mechanical protection.

II. TRANSDUCER FABRICATION

Transducers used in this work were fabricated using the MUMPS multi-user MEMS process on 1 cm² chips using the POLY0 and POLY1 layers. Each transducer consisted of an array of hexagonal units and the upper electrode was released by etching the sacrificial SiO₂ layer through 5 μm square etch holes. An optical micrograph of one of the transducer arrays is shown in Fig. 1.

A range of different transducer designs were studied as indicated in Table I. Transducer design A was the same design previously used to explore coupling to a solid medium [5] and had a POLY0-POLY1 gap of 2.0 μm and relatively high parasitic capacitance between the POLY1 electrode and the substrate. In contrast designs B-F used the DIMPLE mask level to reduce the electrode gap to 1.25 μm and in addition the capacitance between the POLY1 electrode and the substrate were reduced by an improved design for the diaphragm supports. These two changes have the effect of increasing the signal levels observed off-chip.

label	edge [μm]	number	C _d [pF]	C _{stray} [pF]	f _r [kHz]
A	37	180	2.9	150	3470
B	137	95	10.9	80.6	1060
C	157	81	12.2	70.3	812
D1	177	68	13.1	82.4	658
D2	177	68	13.1	69.4	662
E1	207	53	13.9	80.0	482
E2	207	53	13.9	68.9	483
F1	242	36	12.9	74.3	359
F2	242	36	12.9	60.3	366

Table I. Characteristics of transducers used in this work. C_d is the diaphragm capacitance calculated from the layout and C_{stray} is the measured stray capacitance.

Also shown in Table I are the observed resonant frequencies in vacuum. As noted elsewhere, the diaphragms are strongly damped when coupled to solid or liquid media [5]. Consequently these transducers have a broad bandwidth not limited by the diaphragm resonance.

Fabricated and released chips were bonded to a 40-pin ceramic package using silver epoxy. After gold wire bonding, the chip and bond wires were coated using Gelest Zipcone CG silicone (Fig. 2). The thickness of the silicone layer could be controlled to a degree by the amount of silicone which was applied.

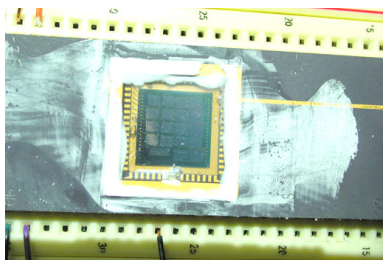


Figure 2. Photograph of chip attached to ceramic package, wire-bonded, and coated with silicone.

III. EFFECT OF COUPLING LAYER

We first consider the effect of the silicone layer thickness on the transducer pulse response. The transducer pulse response is seriously degraded when the silicone layer is several wavelengths in thickness. Figure 3 shows the apparatus used to observe this effect. A commercial PZT transducer (Krautkramer MSW-QC, 5 MHz) driven by a Krautkramer USPC-2100 pulser/ display unit was used to create short ultrasonic pulses. The pulse was transmitted through water between the emitting and receiving transducers. The path length in water was varied from about 0.5 cm to 1.5 cm. The signal received by the cMUT was measured and stored using an oscilloscope as previously reported [5].

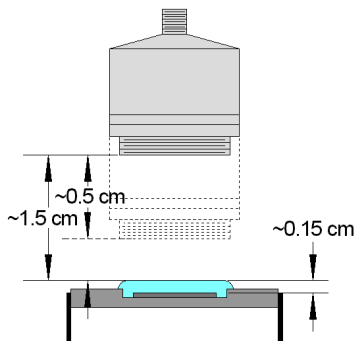


Fig. 3. Arrangement for measurements with water coupling.

Figure 4 shows the transients observed by the cMUT and also the reflected signal detected by the PZT transducer. In this figure the exciting pulse occurred at $t = 5 \mu\text{s}$. The exciting pulse is marked both on the PZT trace (where the small amplitude is a consequence of gating) and on the cMUT trace (because of stray electrical coupling). Signals for two different path lengths are shown (0.5 cm and 1.5 cm). The time difference between the exciting pulse and the first reflection observed by the PZT transducer agrees with the expected delay time $T = d/c$ for the path length d in water with velocity c . Note that the cMUT transducer receives two pulses at approximately $T/2 + 5 \mu\text{s}$. The separation between these two pulses is independent of the path length d .

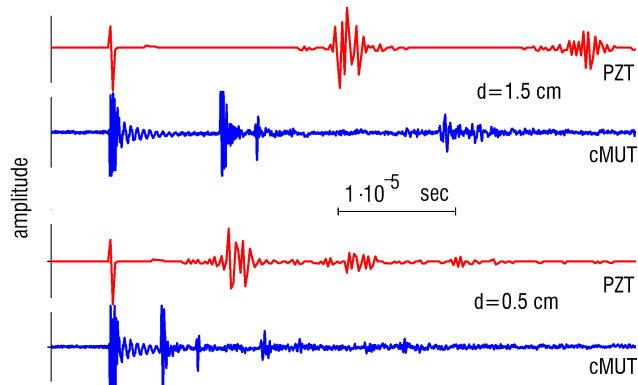


Fig. 4. Demonstration of liquid coupling with thick (~ 0.15 cm) silicone layer: (top) 1.5 cm water path length and (bottom) 0.5 cm water path length. The exciting pulse was at $t = 5 \mu\text{s}$. The red traces show the reflected pulses received by the PZT transducer and the blue traces show the signal observed by the cMUT.

Figure 5 shows a transmission line model for the pulse propagation. In this diagram Z_m is the acoustic impedance of water and Z_c is the acoustic impedance of the silicone layer. To a good approximation, the acoustic impedance of the cMUT transducer Z_t is much less than the impedance of either water or silicone. Consequently we attribute the second pulse of the pair received by the cMUT to reflections within the silicone layer.

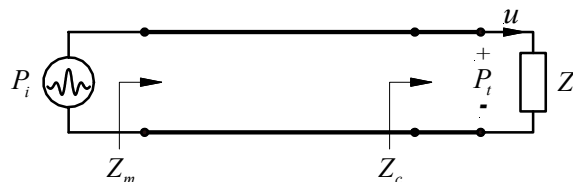


Fig. 5. Transmission line equivalent circuit. Z_m , Z_c , and Z_t represent the acoustic impedances of the water transmission medium, the silicone coating, and the transducer, respectively.

The expected delay for a pulse reflecting from the transducer, traveling through the silicone and reflecting again at the silicone-water interface is given by $\Delta t = 2t_{\text{silicone}}/c_{\text{silicone}}$. We have previously measured the silicone acoustic properties as $c_{\text{silicone}} = 1.3 \times 10^5$ cm/sec and $Z_{\text{silicone}} = 1.5 \times 10^5$ gm/cm²·sec [5]. Based on the observed delay time of 2.4 μ s, we calculate a silicone thickness of 0.16 cm, in good agreement with the measured dimensions. However, the silicone acoustic impedance we reported previously is very close to the acoustic impedance of water (1.48×10^5 gm/cm²·sec). Equal acoustic impedances for silicone and water would result in no reflection at the silicone-water interface.

We have explored this further by using a circuit simulator to model the acoustic propagation. Figure 6 shows the equivalent circuit model. The water transmission medium and the silicone coating were modeled as lossless transmission lines, and the MEMS transducer electrical equivalent circuit was as previously reported [7]. Transient simulations were performed using the circuit simulator PSpice.

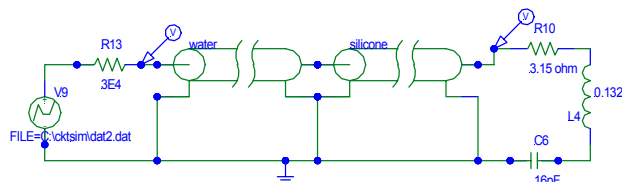


Fig. 6. Circuit for simulation of acoustic propagation using SPICE.

Simulations were performed using as an input a short pulse (width approximately 0.6 μ s) with a center frequency of 5 MHz. The calculations showed only a single pulse detected at the transducer with $Z_{\text{silicone}} = 1.5 \times 10^5$ gm/cm²·sec, while a pulse of approximately the expected magnitude was observed if the silicone acoustic impedance was increased to $Z_{\text{silicone}} = 2.0 \times 10^5$ gm/cm²·sec (Fig. 7). We conclude that the silicone acoustic impedance in these devices is significantly different from that reported previously. Errors in our previous measurement of acoustic impedance do not appear to be large enough to account for this difference; possibly there are differences in the acoustic impedance due to differences in drying for thin layers and bulk specimens of silicone. It should be noted that plastics and rubbers have acoustic impedances in the range $2\text{-}3 \times 10^5$ gm/cm²·sec [8].

We next present there results from a chip containing detectors B-F. A thinner silicone layer was used so that these results show improved pulse response. In addition we obtain an indication of the yield of the silicone coating process.

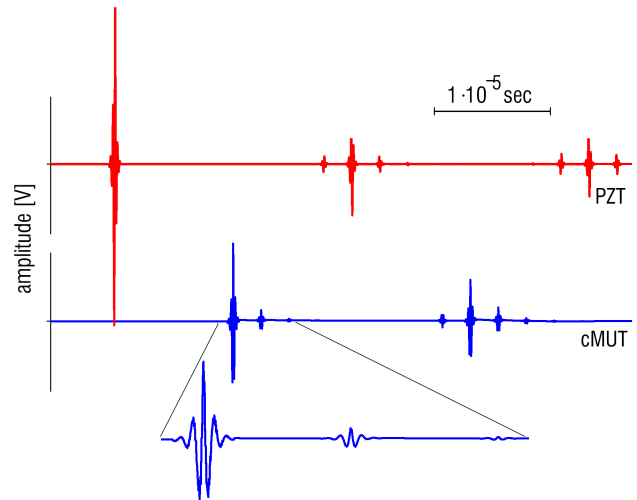


Fig. 7. Simulated signals observed at (top) PZT emitter and (bottom) cMUT receiver. The silicone thickness was 0.15 cm and the silicone acoustic impedance was 2.0×10^5 gm/cm²·sec.

Figure 8 shows the pulse reception for all eight detectors B-F. All detectors survived the coating process and continued to work during two days of continuous exposure to water. Note that the diaphragms are considerably larger than those of transducer A; fragility of these larger diaphragms is evidently not a problem. Signal levels are comparable to those observed with transducer A despite the use of smaller DC bias voltages (10 V vs. 100 V). This is a consequence of the improved design which provides a small gap and reduced parasitic capacitance. We also observe considerably improved pulse shape. There is some broadening compared to the emitted pulse but spurious pulses are absent. This is consistent with circuit simulations which show some broadening for a silicone thickness of 0.026 cm and essentially no broadening for a thickness of 0.006 cm.

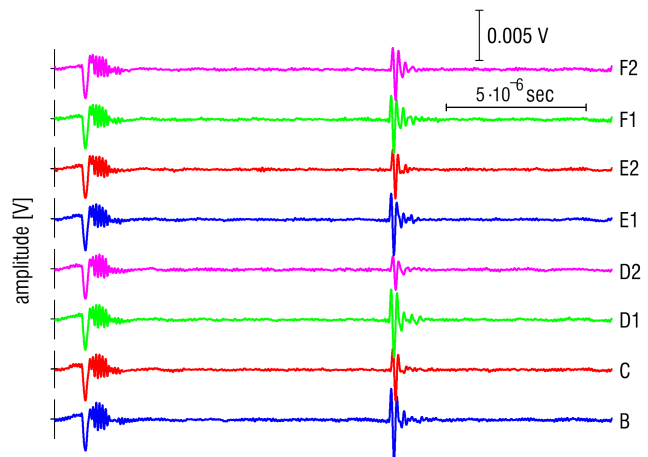


Fig. 8. Measured transients for transducers B-F (10 V bias)

Figure 8 also shows essentially the same behavior for all transducers regardless of diaphragm size. This is exactly as expected given the relative magnitudes of the diaphragm and silicone acoustic impedances.

While these transducers do work effectively as receivers, they are less useful as transmitters. Figure 9 shows operation of a transducer as a transmitter. The emitted pulse can be readily detected by a commercial PZT transducer operated as a receiver. However, reflected pulses are not detectable with a cMUT transducer.

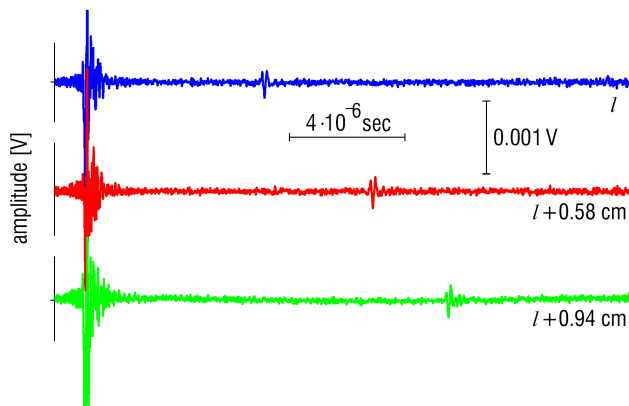


Fig. 9. Signal received by PZT transducer with cMUT used as emitter. The pulse delay increases as the separation between transducers is increased.

IV. TRANSDUCER ROBUSTNESS

As noted earlier, robustness of cMUT transducers is a major concern in applications. Silicone coating appears to considerably reduce the fragility of transducers. The type A transducer reported above survived 1 kg/cm² applied directly above the transducer with a 0.6 cm diameter flat-bottomed rod.

V. ACKNOWLEDGEMENTS

This work is supported by the National Science Foundation under grant CMS-0329880 and by the Commonwealth of Pennsylvania through the Pennsylvania Infrastructure Technology Alliance program. The authors would also like to acknowledge gifts from Krautkramer Inc.

VI. REFERENCES

- [1] "Surface micromachined ultrasound transducers in CMOS technology," P.-C. Eccardt, K. Niederer, T. Scheiter, and C. Hierold, 1996 IEEE Ultrasonics Symposium, pp. 959-962 (1996).
- [2] "Micromachined ultrasonic capacitance transducers for immersion applications," A.G. Bashford, D.W. Schindel, D.A. Hutchins, IEEE Transactions on Ultrasonics, Ferroelectrics, and Frequency Control, vol. 45, pp. 367-375 (1998).
- [3] "Characterization of one-dimensional capacitive micromachined ultrasonic immersion transducer arrays," X. Jin, I. Ladabaum, F.L. Degertekin, S. Calmes, and B.T. Khuri-Yakub, IEEE Journal of Microelectromechanical Systems, vol. 8, pp. 100-114 (1999).
- [4] X. Jin, O. Oralkan, F.L. Degertekin, and B.T. Khuri-Yakub, "Characterization of one-dimensional capacitive micromachined ultrasonic immersion transducer arrays," IEEE Transactions on Ultrasonics, Ferroelectrics, and Frequency Control, vol. 48, pp. 750-760 (2001).
- [5] "MEMS Ultrasonic Transducers for the Testing of Solids," I.J. Oppenheim, A. Jain, and D.W. Greve, IEEE Transactions on Ultrasonics, Ferroelectrics, and Frequency Control, vol. 50, pp. 305-311 (2003).
- [6] "MEMS Phased Array Detection in Contact with Solids," D.W. Greve, A. Jain, and I.J. Oppenheim, 2003 IEEE Ultrasonics Symposium, paper 5D-6.
- [7] "Electrical Characterization of Coupled and Uncoupled MEMS Ultrasonic Transducers," I.J. Oppenheim, A. Jain, and D.W. Greve, IEEE Transactions on Ultrasonics, Ferroelectrics, and Frequency Control, vol. 50, pp. 297-304 (2003).
- [8] "Ultrasonic Transducers For Nondestructive Testing," catalog published by Krautkramer, Inc., (April 2001).